

One-Bond ^{13}C – ^1H Spin-Coupling Constants in Aldofuranosyl Rings: Effect of Conformation on Coupling Magnitude[†]

Anthony S. Serianni,^{*,‡} Jian Wu,[§] and Ian Carmichael^{||}

Contribution from the Department of Chemistry and Biochemistry and Radiation Laboratory, University of Notre Dame, Notre Dame, Indiana 46556, and Department of Chemistry, Purdue University, West Lafayette, Indiana 47907

Received February 13, 1995[⊗]

Abstract: One-bond ^{13}C – ^1H spin-coupling constants ($^1J_{\text{CH}}$) have been studied in the model furanose 2-deoxy- β -D-glycero-tetrofuranose (**1**) as a function of ring geometry in order to assess their utility as conformational probes. *Ab initio* molecular orbital (MO) calculations were conducted on the ten envelope forms and the planar form of **1** using the second-order Møller–Plesset (MP2) electron correlation treatment with a polarized split-valence (6-31G*) basis set. The derived structures were used to compute $^1J_{\text{CH}}$ values in conformers of **1** at the Hartree–Fock and MP2 levels of theory which were subsequently scaled using a factor derived from accurate quadratic configuration interaction (QCISD) calculations. MO results indicate that C–H bond lengths in **1** vary with ring geometry, with a given C–H bond longest when quasi-axial and shortest when quasi-equatorial. Computed $^1J_{\text{CH}}$ values were found to be sensitive to C–H bond orientation, with greater couplings observed when a C–H bond is quasi-equatorial. Computations conducted on β -D-ribofuranose (**3**) and 2-deoxy- β -D-erythro-pentofuranose (**4**) (HF/6-31G* level) show a C–H bond length/orientation dependence similar to that observed in **1**. Experimental (NMR) data are presented which support the proposed correlation. These results suggest a role for $^1J_{\text{CH}}$ in the conformational analysis of furanose rings which may complement current methods based on $^3J_{\text{HH}}$, $^3J_{\text{CH}}$, and $^2J_{\text{CH}}$ values.

Introduction

One-bond ^{13}C – ^1H spin-coupling constants ($^1J_{\text{CH}}$) have been found to be valuable configurational and conformational probes in carbohydrates. For example, Bock and Pedersen^{1–3} have shown that the magnitude of $^1J_{\text{CH}}$ values in aldopyranosyl rings depends on the orientation of the C–H bond and the number of electronegative substituents attached to the coupled carbon. Thus, $^1J_{\text{C1,H1}} = 170.1$ Hz in methyl α -D-glucopyranoside (C1–H1 bond equatorial) and 161.3 Hz in methyl β -D-glucopyranoside (C1–H1 bond axial), whereas $^1J_{\text{C2,H2}} = \sim 145.5$ Hz in both anomers (C2–H2 bond axial). The dependence of $^1J_{\text{C1,H1}}$ on anomeric configuration has proven valuable in assigning linkage configuration in oligosaccharides,^{4,5} and recent work by Tvaroska and co-workers^{6,7} indicates that $^1J_{\text{CH}}$ in oligosaccharides may be sensitive to *O*-glycoside linkage conformation.

In contrast to aldopyranosyl rings, the behavior of $^1J_{\text{CH}}$ values in aldofuranosyl rings has not been well studied, mainly because considerable conformational flexibility of these rings in solution complicates their interpretation. However, the effort required to better understand $^1J_{\text{CH}}$ in these structures can be justified on

the following grounds. Firstly, $^1J_{\text{CH}}$ values, being large compared to $^3J_{\text{HH}}$, $^2J_{\text{CH}}$, and $^3J_{\text{CH}}$ values, are potentially attractive structural probes in larger biomolecules (e.g., oligonucleotides) where they should be measured more easily than the latter. Secondly, given the conformational flexibility of furanose rings and the wide number of potential conformational models available to them, it is desirable to access as many experimental NMR parameters as possible in order to test the validity of particular models. $^1J_{\text{CH}}$ data could thus provide additional information to facilitate this process. Such an application was suggested recently by Varani and Tinoco,⁸ who reported a dependence of $^1J_{\text{CH}}$ on β -D-ribofuranosyl ring conformation in an RNA oligomer, although a structural rationale for the observed effects was not proposed.

We present in this paper experimental and computational data which may shed some light on the relationship between furanose ring conformation and $^1J_{\text{CH}}$. Specifically, we have conducted *ab initio* molecular orbital calculations on ten nonplanar (envelope) forms and the planar form of 2-deoxy- β -D-glycero-tetrofuranose (**1**), a structural analog of the 2-deoxy- β -D-erythro-

[†] This is Document No. NDRL-3668 from the Notre Dame Radiation Laboratory.

[‡] Department of Chemistry and Biochemistry, University of Notre Dame.

[§] Purdue University.

^{||} Radiation Laboratory, University of Notre Dame.

* Corresponding author.

[⊗] Abstract published in *Advance ACS Abstracts*, July 15, 1995.

(1) Bock, K.; Lundt, I.; Pedersen, C. *Tetrahedron Lett.* **1973**, 1037.

(2) Bock, K.; Pedersen, C. *J. Chem. Soc., Perkin Trans. 2* **1974**, 293.

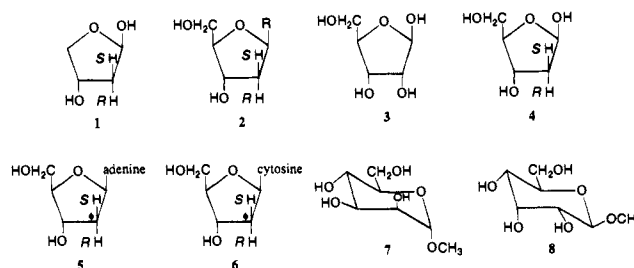
(3) Bock, K.; Pedersen, C. *Acta Chem. Scand.* **1975**, B29, 258.

(4) Nunez, H. A.; Barker, R. *Biochemistry* **1980**, *19*, 489.

(5) Rosevear, P. R.; Nunez, H. A.; Barker, R. *Biochemistry* **1982**, *21*, 1421.

(6) Tvaroska, I.; Kozar, T.; Hricovini, M. Oligosaccharides in Solution—Conformational Analysis by NMR Spectroscopy and Calculation. In *Computer Modeling of Carbohydrate Molecules*; French, A. D., Brady, J. W., Eds.; ACS Symposium Series 430; American Chemical Society: Washington, DC, 1990; pp 162–176.

(7) Tvaroska, I. *Carbohydr. Res.* **1990**, *206*, 55.



pentofuranosyl ring (**2**) found in DNA, from which C–H bond lengths were predicted as a function of ring shape. Similar but less rigorous computational results are also presented for the more biologically-relevant β -D-ribofuranose (**3**) and 2-deoxy-

(8) Varani, G.; Tinoco, I., Jr. *J. Am. Chem. Soc.* **1991**, *113*, 9349.

β -D-erythro-pentofuranose (**4**) rings. The predicted bond lengths in **1** were used to compute $^1J_{CH}$ values for each carbon of **1** as a function of ring conformation, revealing a consistent relationship between C–H bond orientation (quasi-axial or quasi-equatorial) and coupling magnitude. We then describe some experimental results, using several model systems, that provide some verification of the computational predictions.

Experimental Section

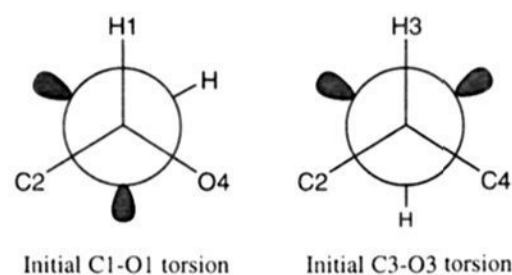
Compounds. [2'- ^{13}C]2'-Deoxyadenosine and [2'- ^{13}C]2'-deoxycytidine were prepared from [2'- ^{13}C]adenosine and [2'- ^{13}C]cytidine, respectively, as described previously.^{9,10} Methyl α -D-[1- ^{13}C]mannopyranoside, methyl α -D-[2- ^{13}C]mannopyranoside, methyl α -D-[3- ^{13}C]mannopyranoside, methyl β -D-[1- ^{13}C]allopentopyranoside, methyl β -D-[2- ^{13}C]allopentopyranoside, and methyl β -D-[3- ^{13}C]allopentopyranoside were prepared by methods described previously,^{11–13} and only a brief account of the procedures is described here. D-[1- ^{13}C]Mannose and D-[1- ^{13}C]allose were synthesized from D-pentoses (D-arabinose and D-ribose) and $K^{13}CN$ by cyanohydrin reduction;¹¹ D-[1- ^{13}C]glucose and D-[1- ^{13}C]altrose were obtained, respectively, as byproducts of these reactions. D-[2- ^{13}C]Mannose and D-[2- ^{13}C]allose were prepared from the latter byproducts by molybdate-catalyzed epimerization.¹⁴ D-[3- ^{13}C]Mannose and D-[3- ^{13}C]allose were prepared from D-[2- ^{13}C]arabinose¹³ and D-[2- ^{13}C]ribose,¹³ respectively, and KCN by cyanohydrin reduction.¹¹ Methyl glycosidation was achieved by the Fischer method using Dowex 50 (H^+) resin as the catalyst,¹⁵ and purification of specific anomers was achieved by chromatography on Dowex 1 \times 8 (200–400 mesh) in the OH^- form.¹⁶

NMR Spectroscopy. 1D 1H NMR spectra were obtained on Varian VXR-500S (UNITY) (methyl aldopyranosides) and Varian VXR-600 (UNITY) (2'-deoxyribonucleosides) FT-NMR spectrometers. Spectra were collected at $\sim 30^\circ C$ and were processed with resolution enhancement to optimize the measurement of spin-coupling constants.

Computational Methods. All structural studies were performed using the Gaussian 92 series of programs [G92]¹⁷ by employing the standard 6-31G* split-valence basis set with polarization (*d*) functions¹⁸ on carbon and oxygen. Geometries were first optimized at the Hartree–Fock level and subsequently refined using second-order Møller–Plesset perturbation theory.

One-bond ^{13}C – 1H spin-coupling constants ($^1J_{CH}$) were determined by finite-field perturbation theory using a modified version of the Gaussian suite¹⁹ and a basis set, denoted [5s2p1d|2s], as described earlier.¹⁹ Only the contact component, which is known to dominate the indirect spin–spin interaction, was recovered. At the HF level, the predicted $^1J_{CH}$ values are typically much larger than those observed experimentally since correlation effects are not included at this level of theory. The most straightforward (and tractable) approach to introduce these important correlation corrections involves the MP2 procedure. Unfortunately, calculations of $^1J_{CH}$ values at this level typically overestimate the magnitude of these corrections. To address this problem, two specific $^1J_{CH}$ values were determined using a more

Chart 1



thorough treatment of the effects of electron correlation by the quadratic configuration interaction method²⁰ (QCISD). A factor, *f*, for scaling the MP2 estimates of the correlation effects on $^1J_{CH}$ values in the above basis set was determined from the relationship $f = [^1J_{CH}(QCISD) - ^1J_{CH}(HF)]/[^1J_{CH}(MP2) - ^1J_{CH}(HF)] \approx 0.83$. For example, for $^1J_{C1,H1}$ in the 0E conformer of **1**, we compute $^1J_{CH}(HF) = 194.7$ Hz, $^1J_{CH}(MP2) = 143.4$ Hz, and $^1J_{CH}(QCISD) = 152.0$ Hz.

A similar scaling procedure was demonstrated recently²¹ to be reliable for the treatment of correlation effects on one-bond ^{13}C – ^{13}C coupling constants ($^1J_{CC}$). Calculations of $^1J_{CH}$ values at the QCISD/[521|2] level in ethane, ethanol, and ethylene glycol produce the same scaling factor and underestimate experimental $^1J_{CH}$ values by about 6%. A similar shortfall is thus expected here.

Results and Discussion

A. Validation of the Computational Model. Geometric optimizations of all molecular parameters (i.e., bond lengths, angles, torsions) in ten envelope (E) forms and the planar (P) form of **1** were conducted with the exception of one endocyclic torsion in E forms (two in the P form) which was (were) fixed at 0° to constrain the calculation to a specific conformer.²² In computations with HF/6-31G* and MP2/6-31G* methods, exocyclic C1–O1 and C3–O3 torsions were set at the initial values shown in Chart 1. Rotation about these bonds effects the conformational energies of **1**, especially the C1–O1 torsion where the exoanomeric effect²³ operates. The initial C1–O1 torsion was therefore chosen to optimize the latter effect (OH-1 gauche to H-1 and the ring oxygen O4; Chart 1), whereas the C3–O3 torsion was chosen somewhat arbitrarily; however, both torsions were allowed to relax during optimization. A more comprehensive treatment of the effects of exocyclic C–O torsions on the structures and conformational energies of **1** will be reported elsewhere, and only specific aspects of these effects that bear on the main arguments of this paper are presented below.

Conformational energy profiles obtained from HF/6-31G* and MP2/6-31G* calculations are shown in Figure 1. Both data sets are consistent with a pseudorotational mechanism²⁴ of conformer interconversion, with the global energy minimum at 4E (a south (S) form) and a local minimum at E_2 (a north (N) form). This result provides some validation of the computational method, as nonplanar furanose conformers are commonly considered to exchange via pseudorotation.²⁴ MP2/6-31G* conformational energies (kcal/mol) for the E forms of **1** are as follows: 3E , 1.5; E_4 , 3.2; 0E , 3.9; E_1 , 3.9; 2E , 3.0; E_3 , 1.4; 4E , 0.0; E_0 , 0.55; 1E , 0.58; E_2 , 0.43. Interconversion between 4E and E_2 occurs mainly via west (e.g., E_0) forms. In contrast,

(9) Kline, P. C.; Serianni, A. S. *Magn. Reson. Chem.* **1990**, *28*, 324.

(10) Bandyopadhyay, T.; Wu, J.; Serianni, A. S. *J. Org. Chem.* **1993**, *58*, 5513.

(11) Serianni, A. S.; Nunez, H. A.; Barker, R. *Carbohydr. Res.* **1979**, *72*, 71.

(12) Serianni, A. S.; Vuorinen, T.; Bondo, P. B. *J. Carbohydr. Chem.* **1990**, *9*, 513.

(13) Serianni, A. S.; Bondo, P. B. *J. Biomol. Struct. Dyn.* **1994**, *11*, 1133.

(14) Hayes, M. L.; Pennings, N. J.; Serianni, A. S.; Barker, R. *J. Am. Chem. Soc.* **1982**, *104*, 6764.

(15) Podlasek, C. A.; Wu, J.; Stripe, W. A.; Bondo, P. B.; Serianni, A. S. *J. Am. Chem. Soc.* **1995**, in press.

(16) Austin, P. W.; Hardy, F. E.; Buchanan, J. C.; Baddiley, J. *J. Chem. Soc.* **1963**, 5350.

(17) Frisch, M. J.; Trucks, G. W.; Head-Gordon, M.; Gill, P. M. W.; Wong, M. W.; Foresman, J. B.; Johnson, B. G.; Schlegel, H. B.; Robb, M. A.; Replogle, E. S.; Gomperts, R.; Andres, J. L.; Raghavachari, K.; Binkley, J. S.; Gonzales, C.; Martin, R. L.; Fox, D. J.; DeFrees, D. J.; Baker, J.; Stewart, J. J. P.; Pople, J. A. *Gaussian 92*, Revision C.3; Gaussian, Inc.: Pittsburgh, PA, 1992.

(18) Hariharan, P. C.; Pople, J. A. *Chem. Phys. Lett.* **1972**, *16*, 217.

(19) Carmichael, I. *J. Phys. Chem.* **1993**, *97*, 1789.

(20) Pople, J. A.; Head-Gordon, M.; Raghavachari, K. *J. Chem. Phys.* **1987**, *87*, 5968.

(21) Carmichael, I.; Chipman, D. M.; Podlasek, C. A.; Serianni, A. S. *J. Am. Chem. Soc.* **1993**, *115*, 10863.

(22) (a) Serianni, A. S.; Chipman, D. M. *J. Am. Chem. Soc.* **1987**, *109*, 5297. (b) Garrett, E. C.; Serianni, A. S. In *Computer Modeling of Carbohydrate Molecules*; French, A. D., Brady, J. W., Eds.; ACS Symposium Series 430; American Chemical Society: Washington, DC, 1990; pp 91–119. (c) Garrett, E. C.; Serianni, A. S. *Carbohydr. Res.* **1990**, *206*, 183.

(23) Lemieux, R. U. *Pure Appl. Chem.* **1971**, *25*, 527.

(24) Altona, C.; Sundaralingam, M. *J. Am. Chem. Soc.* **1972**, *94*, 8205.

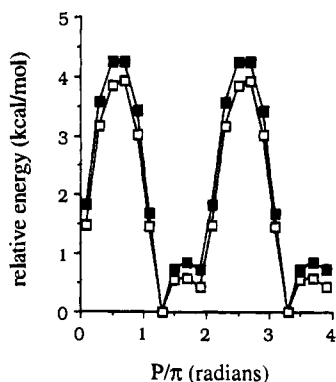


Figure 1. Conformational energies of the nonplanar forms of **1** determined by *ab initio* MO calculations using HF/6-31G* (closed squares) and MP2/6-31G* (open squares) levels. Data are shown for two cycles of the pseudorotational itinerary;²⁴ $0.1 P/\pi = {}^3E$.

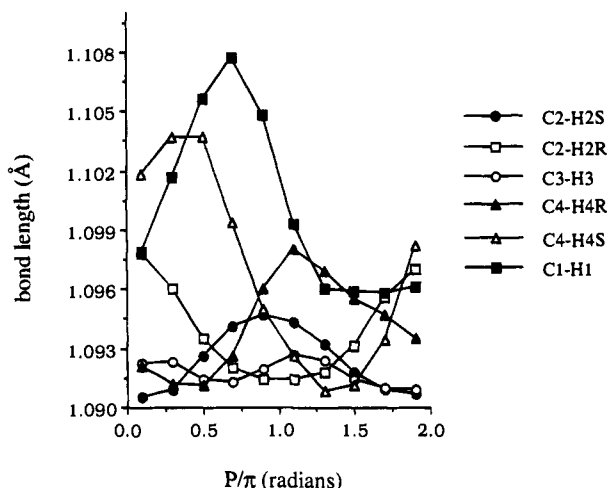


Figure 2. Effect of ring conformation on the six C-H bond lengths in **1** ($0-2.0 P/\pi$ represents one full cycle of the pseudorotational itinerary;²⁴ $0.1 P/\pi = {}^3E$).

N/S interconversion for **2** occurs mainly via east (e.g., 0E) forms.²⁵ Thus, the absence of a bulky exocyclic CH_2OH group at C4 of **1** apparently eliminates the steric crowding between substituents at C1 and C4 that occurs in E_0 of **2** and destabilizes this conformer relative to 0E . The west pathway for N/S interconversion of **1** is probably further reinforced by stereo-electronic effects. In west forms of **1**, gauche effects²⁶ involving the ring oxygen (O4) and O3 are optimized (O3 and O4 are gauche) and C1-O1 bond orientation (quasi-axial or nearly so) is optimized by the anomeric effect.²⁷ Both provide stabilizing forces that are either absent or reduced in strength in east forms of **1**.

B. Computed C-H Bond Lengths in 1. A plot of the six C-H bond lengths in **1** as a function of ring conformation, using data obtained from MP2/6-31G* calculations, is shown in Figure 2. These data reveal that C-H bond lengths in **1** depend on ring shape; in general, a given C-H bond is longest when quasi-axial and shortest when quasi-equatorial, although the magnitude of change varies with each bond. The behavior of the C3-H3 bond length appears to deviate from this general rule, however, being relatively insensitive to ring shape, suggesting that factors in addition to bond orientation affect C-H bond

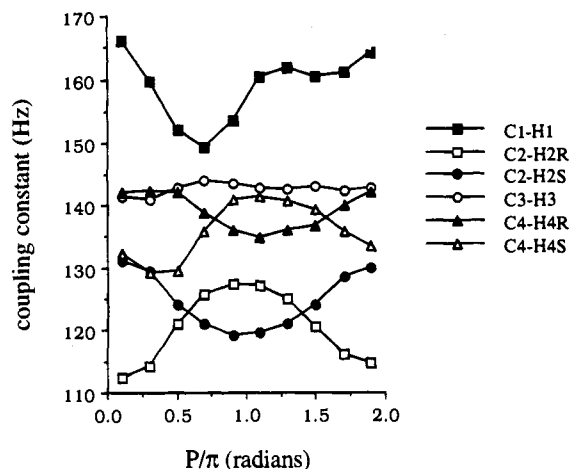


Figure 3. ${}^1J_{\text{CH}}$ values computed for each C-H bond in **1** as a function of ring conformation ($0.1 P/\pi = {}^3E$). Couplings are scaled from calculated HF and MP2 values (see text).

length in these rings. Some of these factors are considered below.

Recalling the approximate relationship between ${}^1J_{\text{CH}}$ and s character of the C-H bond, namely ${}^1J_{\text{CH}} = 500 (\%S_{\text{CH}})$, proposed by Müller and Pritchard,²⁸ it may be argued that axial C-H bonds, being longer and thus presumably having less s character, should yield smaller ${}^1J_{\text{CH}}$ values than equatorial C-H bonds, in agreement with prior findings in aldopyranosyl rings.¹⁻³ To explore this potential dependency further, ${}^1J_{\text{CH}}$ values were computed at the Hartree-Fock (HF) level by using the MP2/6-31G*-optimized geometric parameters obtained for each envelope form of **1** and employing a basis set ([5s2p1d|2s]) and a calculational method described previously,¹⁹ and scaled as described below (Figure 3). These data show that the computed ${}^1J_{\text{CH}}$ follow the orientational effects on C-H bond lengths deduced above from considerations of s-character. Thus, for example, the conversion of E_2 (N form) to 2E (S form) results in a decrease in ${}^1J_{\text{C2,H2S}}$ and an increase in ${}^1J_{\text{C2,H2R}}$, since the C2-H2S bond lengthens (changes from quasi-equatorial to quasi-axial) and the C2-H2R bond shortens (changes from quasi-axial to quasi-equatorial).

While the general trends in ${}^1J_{\text{CH}}$ values predicted from these calculations can be considered reliable, we found that ${}^1J_{\text{CH}}$ values computed at the HF level of theory were significantly larger than expected experimental values. We have shown elsewhere¹⁹ that MP2-correlated calculations of spin-coupling constants "overcorrect" the HF values for ${}^1J_{\text{CC}}$, when compared to results from the more extensive and reliable quadratic configuration interaction (QCISD) treatment of electron correlation effects. Similar behavior is expected for ${}^1J_{\text{CH}}$. As indicated above, the QCISD-derived ${}^1J_{\text{CH}}$ values in this paper were obtained by a scaling procedure analogous to that outlined previously for ${}^1J_{\text{CC}}$.²¹ This scaling method, however, does not take solvent effects into consideration, which can be significant for ${}^1J_{\text{CH}}$.²⁹ At the present time, it is not possible to include solvent contributions to ${}^1J_{\text{CH}}$ in a reliable *ab initio* fashion.

C. Extensions to Biologically-Important Furanose Rings. The effect of C-H bond orientation on C-H bond length was also examined in more biologically-relevant aldofuranose rings. *Ab initio* MO computations conducted on β -D-ribofuranose (**3**) (Figure 4) and 2-deoxy- β -D-erythro-pentofuranose (**4**) (data not shown) at the HF/6-31G* level reveal C-H bond length dependencies on bond orientation similar to those observed in **1**. We therefore conclude that the behavior of ${}^1J_{\text{CH}}$ values in **3** and **4** should be similar to that found in **1**.

(25) Saenger, W. *Principles of Nucleic Acid Structure*; Springer-Verlag: New York, 1984; pp 55-65.

(26) Wolfe, S. *Acc. Chem. Res.* **1972**, *5*, 102.

(27) Lemieux, R. U. In *Molecular Rearrangements*; de Mayo, P., Ed.; Wiley-Interscience: New York, 1963; p 713.

(28) Müller, N.; Pritchard, D. E. *J. Chem. Phys.* **1959**, *31*, 768.

(29) Bock, K.; Pedersen, C. *Carbohydr. Res.* **1979**, *71*, 319.

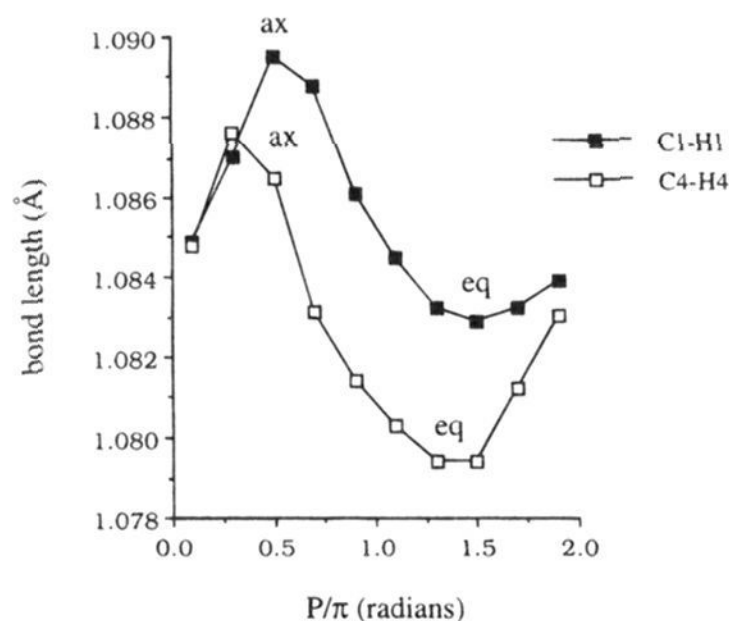


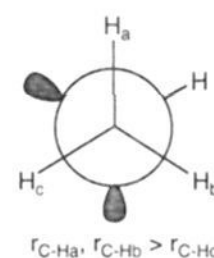
Figure 4. Effect of ring conformation on the C1–H1 and C4–H4 bond lengths in β -D-ribofuranose (**3**) ($0.1 P/\pi = {}^3E$) (ax = quasi-axial; eq = quasi-equatorial)

D. Experimental Verification. Experimental verification of the conformational dependence of ${}^1J_{CH}$ values in aldofuranosyl rings is difficult to obtain given the inherent flexibility of these rings in solution. The traditional approach of using conformationally-constrained model systems for this purpose is subject to errors caused by substitution and/or ring-strain effects. Faced with these limitations, we adopted three approaches: (a) examine ${}^1J_{CH}$ values in the furanose ring of nucleosides whose conformational behavior is reasonably well defined, (b) examine ${}^1J_{CH}$ values in conformationally-rigid non-furanose rings containing coupling fragments related structurally to those found in specific furanose conformers, and (c) examine previously-reported ${}^1J_{CH}$ values in conformationally-constrained oligonucleotides.

${}^1J_{CH}$ Values in 2'-Deoxyribonucleosides. 2'-Deoxyadenosine (**5**) and 2'-deoxycytidine (**6**) were prepared^{9,10,13,30} singly-labeled with ${}^{13}C$ at C2', and accurate ${}^1J_{CH}$ values at C2' were obtained via their 1H NMR spectra (600 MHz). In **5**, ${}^1J_{C2',H2'S} = 133.3$ and ${}^1J_{C2',H2'R} = 136.6$ Hz, whereas ${}^1J_{C2',H2'S} = 133.7$ and ${}^1J_{C2',H2'R} = 135.8$ Hz in **6**. Thus, in both **5** and **6**, ${}^1J_{C2',H2'R} > {}^1J_{C2',H2'S}$, with observed differences of 3.3 and 2.1 Hz, respectively. A two-state N/S equilibrium is generally invoked to describe the conformational behavior of the furanose rings in **5** and **6**,²⁵ and an analysis of ${}^3J_{HH}$ and longer-range J_{CH} values in these rings¹⁰ indicates a preference for S conformations (e.g., 2E). In S forms, the C2'–H2'S bond is quasi-axial, whereas the C2'–H2'R bond is quasi-equatorial. Thus, based on the above ${}^1J_{CH}$ correlations, $J_{C2',H2'R}$ is predicted to be greater than ${}^1J_{C2',H2'S}$, in agreement with observation. The difference between $J_{C2',H2'R}$ and ${}^1J_{C2',H2'S}$ is not as large as might be expected due to the presence of N/S conformational averaging in solution. This difference also depends on the specific N and S conformers in chemical exchange (Figure 3).

β -D-Ribofuranose Models. Changes in the magnitudes of ${}^1J_{CH}$ values as a function of conformation in **3** may be estimated by examining aldopyranosyl rings having configurations mimicking those found in discrete conformers. Thus, an examination of the α -manno configuration reveals a relative disposition of electronegative substituents at C1, C2, and C3 (axial–axial–equatorial, respectively) similar to that found in N conformers of **3**. Likewise, the relative orientation of substituents in the β -allo configuration (equatorial–equatorial–axial, respectively) mimics that found in S conformers of **3**. Thus, ${}^1J_{C1,H1}$, ${}^1J_{C2,H2}$,

Chart 2



and ${}^1J_{C3,H3}$ values in these model aldopyranosyl rings may be used to approximate the effect of furanose ring geometry on ${}^1J_{CH}$ values.

${}^1J_{C1,H1}$ in methyl α -D-mannopyranoside (**7**) and methyl β -D-allopyranoside (**8**) are 171.0 and 163.4 Hz, respectively. ${}^1J_{C2,H2} = 148.5$ and 143.8 Hz whereas ${}^1J_{C3,H3} = 146.5$ and 149.8 Hz in **7** and **8**, respectively. Within each pair, the larger coupling is associated with the equatorial C–H bond, again consistent with the computational predictions. It should, however, be appreciated that **7** and **8** are imperfect mimics of N and S forms of **3**, since the geometries about C1, C2, and C3 of **7** and **8** are not identical to those at corresponding carbons in these furanose forms. Nevertheless, this comparison provides a rough estimate of the magnitude of change to be expected in ${}^1J_{CH}$ values as particular C–H bonds in **3** experience a change in orientation.

${}^1J_{CH}$ Values in RNA Oligomers. The computational predictions derived in this study also provide an explanation of ${}^1J_{CH}$ data obtained recently by Varani and Tinoco⁸ in specific residues of the RNA oligomer GGACUUCGGUCC. In this 12-mer, ${}^1J_{C2',H2'}$ values were ~ 160 Hz in N conformers and 145–150 Hz in S forms, whereas the opposite was observed for ${}^1J_{C3',H3'}$. Inspection of the β -ribo ring **3** shows that the observed ${}^1J_{C2',H2'}$ and ${}^1J_{C3',H3'}$ values are larger in the form having the quasi-equatorial C–H bond.

E. Other Considerations. Factors in addition to C–H bond orientation probably affect the behavior of ${}^1J_{CH}$ values in aldofuranosyl rings. The computational results presented above show that C–H bond length significantly affects ${}^1J_{CH}$ magnitude, with shorter bonds generating larger ${}^1J_{CH}$. It is likely that lone-pair orbitals play a role in affecting these lengths and thus, indirectly, the magnitude of ${}^1J_{CH}$. Freymann and Gueron³¹ showed over 50 years ago that the two C–H bonds in a given staggered rotamer of methanol which are antiperiplanar to a lone-pair orbital on oxygen are longer (due to lone pair $\rightarrow \sigma^*_{CH}$ interactions) than the remaining C–H bond which is gauche to both lone pairs (Chart 2). A similar effect was observed in our calculations (HF/6-31G*) on β -D-ribofuranose (**3**). Although the same *initial* exocyclic C–O torsions were employed in computations of each envelope form of **3**, the optimized C3–O3 torsion angle changed significantly and systematically through the pseudorotational itinerary, whereas the initial C2–O2 torsion remained relatively unchanged after optimization (Figure 5). The large change in the former is probably driven by H-bonding interactions between the *cis* OH groups at C2 and C3. More importantly, as shown in Figure 6, the effect of C–H bond orientation on C2–H2 bond length is as expected, whereas that for C3–H3 is apparently anomalous (longer when equatorial, *i.e.*, in S forms). The latter behavior may be explained by noting that one of the lone pairs on O3 becomes nearly antiperiplanar to the C3–H3 bond when the latter is quasi-equatorial (due to C3–O3 bond rotation) (Chart 3), and this lone-pair effect apparently supercedes bond orientation factors. The lone-pair effect may also be responsible for the observed effect of *O*-glycoside torsion on ${}^1J_{CH}$ values in oligosaccharides reported recently.^{6,7}

(30) Kline, P. C.; Serianni, A. S. *J. Am. Chem. Soc.* **1990**, *112*, 7373.

(31) Freymann, R.; Gueron, J. C. *R. Acad. Sci.* **1937**, *205*, 859.

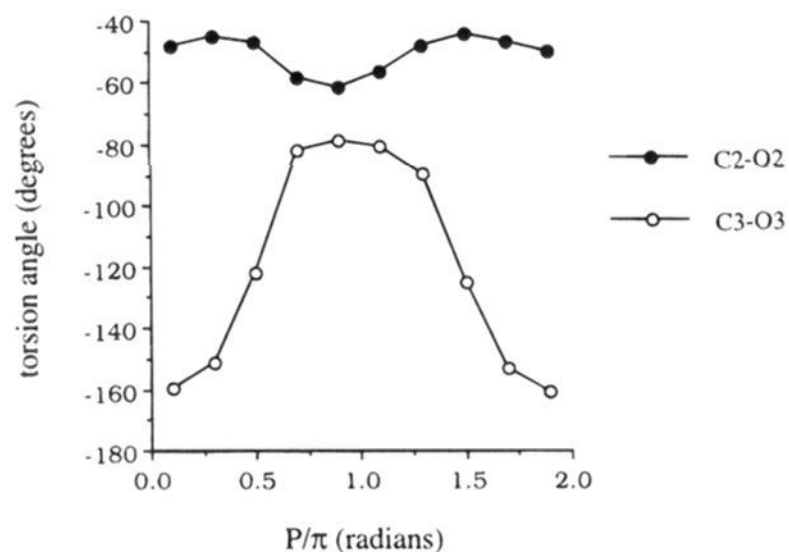


Figure 5. Optimized C2–O2 and C3–O3 bond torsions in the ten nonplanar E forms of β -D-ribofuranose (**3**) ($0.1 P/\pi = {}^3\text{E}$).

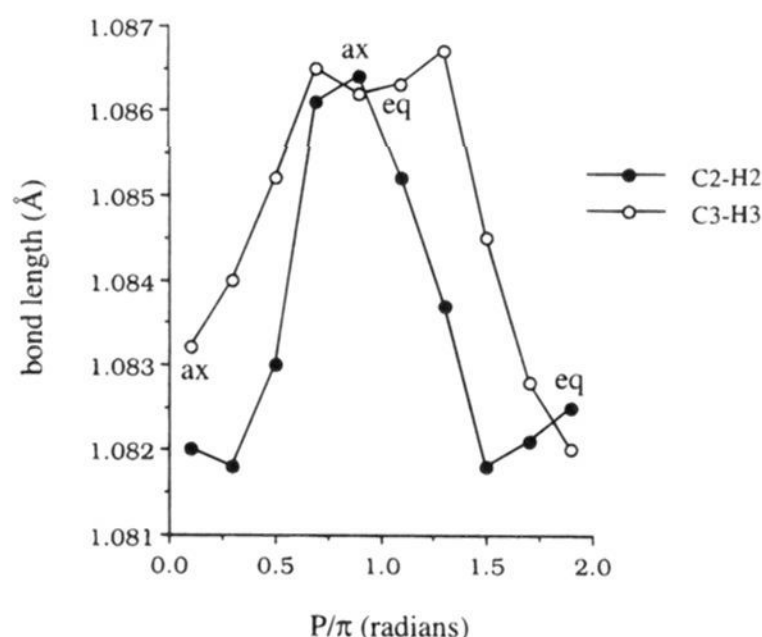
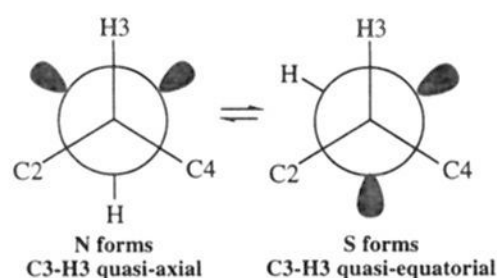


Figure 6. Effect of ring conformation on the C2–H2 and C3–H3 bond lengths in β -D-ribofuranose (**3**) ($0.1 P/\pi = {}^3\text{E}$). (ax = quasi-axial; eq = quasi-equatorial).

Chart 3



The effect of lone pairs on C–H bond lengths may partly explain the different sensitivities of each C–H bond length in **1** to ring conformation. As shown in Figure 2, the C1–H1 and C4–H4S bonds exhibit greater changes in length than the remaining C–H bonds. This different behavior may be attributed to the effect of O4 (ring oxygen) lone pairs. In ring conformations in which the C1–H1 or C4–H4S bonds are quasi-axial, one lone pair on O4 is antiperiplanar to these bonds, thereby enhancing the lengthening (i.e., both orientation and lone-pair effects are operating in concert) (Chart 4). This argument might appear to be compromised by the observed behavior of the C4–H4R bond, which exhibits much less sensitivity to conformation compared to C4–H4S despite the fact that it can also orient antiperiplanar to the “bottom” O4 lone pair in west conformations. However, in these conformations, O1 is nearly quasi-axial, and thus the “bottom” lone-pair on O4 delocalizes into the O4–C1 bond (this delocalization causes the observed shortening of the O4–C1 bond when C1–O1 is quasi-axial), and this competing effect diminishes the anticipated lone-pair effect on C4–H4R (Chart 5).

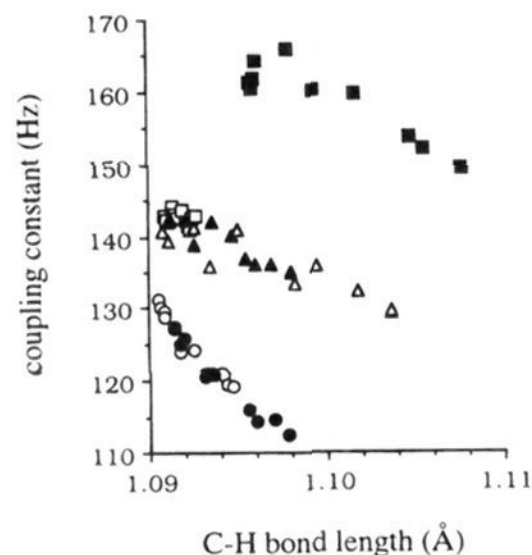


Figure 7. Sensitivity of computed ${}^1J_{\text{CH}}$ values to C–H bond lengths in **1**. Three unique categories are observed: C1–H1, closed squares; C2–H2R, closed circles; C2–H2S, open circles; C3–H3, open squares; C4–H4R, closed triangles; C4–H4S, open triangles.

Chart 4

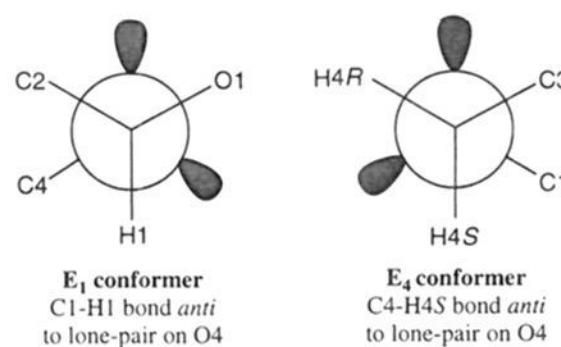
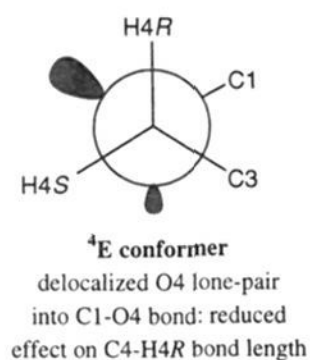


Chart 5



The effects of exocyclic C–O torsions in **1** were examined by systematically inspecting 99 geometrically-optimized conformers (3^2 relative C–O torsions for E and P forms) at a lower level of theory (HF/3–21G). The results showed that, for a given set of C–O torsions, the C–H bond lengths behave consistently (i.e., the longer C–H bond correlates with a quasi-axial orientation). Thus, the expected motional averaging about exocyclic C–O bonds in solution should not negate the correlation, although changes in ${}^1J_{\text{CH}}$ values could be truncated. If, however, a considerable change in the behavior of C–O bonds occurs in different conformations (e.g., free rotation \rightarrow fixed), then the interpretation of ${}^1J_{\text{CH}}$ values in terms of C–H bond orientation can be complicated.

The direct correlation between computed ${}^1J_{\text{CH}}$ values and bond length is shown in Figure 7. These data were obtained from scaled QCISD calculations, although a similar picture also emerges from HF- and MP2-derived values. The coupling constants fall cleanly into three groups depending on the number of electronegative substituents (ring or hydroxylic oxygen) on the coupled carbon. Coupling is largest for the C1–H1 bond (two substituents), intermediate for the C3–H3 and C4–H4 bonds (one substituent), and lowest for the C2–H2 bonds (no substituents). Interestingly, while the slopes of the fit lines are similar for the singly and doubly substituted linkages, that for the unsubstituted case is markedly larger.

Finally, it has been suggested previously³² that bond angle deformation resulting from bond torsion change is responsible for the dependence of $^1J_{C1,H1}$ on the anomeric configuration of aldopyranosyl rings. In this paper, C–H bond lengths are correlated with $^1J_{CH}$ values with the realization that both bond length and bond angle changes are mediated by common stereoelectronic factors.

Conclusions

This paper presents some computational and experimental data aimed at providing a better understanding of the structural dependencies of $^1J_{CH}$ values in aldofuranosyl rings. The computational results suggest a correlation between C–H bond length and C–H bond orientation in these structures, namely, that a given C–H bond is shorter when quasi-equatorial than when quasi-axial. Computed $^1J_{CH}$ values were found to vary

inversely with C–H bond length, permitting a correlation between $^1J_{CH}$ and bond orientation that may be useful in studies of furanosyl ring conformation in solution. Despite the inherent problems associated with interpreting spin-couplings in these flexible rings, some experimental data were obtained which appear to confirm the predicted correlation. While the proposed structural interpretation of $^1J_{CH}$ values requires further validation through experiment, the present results suggest that an integrated analysis of these couplings in furanose rings, such as those found in DNA and RNA, may prove feasible and thus provide valuable conformational information complementary to that obtained from other NMR parameters.

Acknowledgment. The research described herein has been supported by the Office of Basic Energy Sciences of the United States Department of Energy and Omicron Biochemicals, Inc., South Bend, IN.

(32) Gorenstein, D. G. *J. Am. Chem. Soc.* **1977**, *99*, 2254.